Available online at www.sciencedirect.com
SCIENCE DIRECT
Catalysis Today 110 (2005) 221–227
CATALYSIS TODAY
www.elsevier.com/locate/cattod

Reactivity of generated oxygen species from nitrous oxide over [Fe,Al]MFI catalysts for the direct oxidation of benzene to phenol

Jerome B. Taboada [a,*], Emiel J.M. Hensen [b], Isabel W.C.E. Arends [c], Guido Mul [d], Arian R. Overweg [a]

[a] *Department of Radiation, Radionuclides and Reactors, Faculty of Applied Sciences, Delft University of Technology, Mekelweg 15, 2629 JB, Delft, The Netherlands*
[b] *Schuit Institute of Catalysis, Eindhoven University of Technology, P.O. Box 513, 5600 MB, Eindhoven, The Netherlands*
[c] *Section Biocatalysis and Organic Chemistry, Department of Biotechnology, Faculty of Applied Sciences, Delft University of Technology, Julianalaan 136, 2628 BL Delft, The Netherlands*
[d] *Reactor and Catalysis Engineering, DelftChemTech, Faculty of Applied Sciences, Delft University of Technology, Julianalaan 136, 2628 BL Delft, The Netherlands*

Available online 28 October 2005

Abstract

The catalytic performance of various steam-activated [Fe,Al]MFI catalysts in the direct oxidation of benzene to phenol using N_2O as oxidant is described. All [Fe,Al]MFI catalysts contain ca. 90% of iron in the high-spin Fe^{2+} state, independent of the iron concentration (0.075–0.6 wt.% iron). In the presence of N_2O at 623 K, most Fe^{2+} ions (>90%) were oxidized to Fe^{3+} ions as deduced from Mössbauer spectroscopy. In the presence of benzene, subsequent reduction of Fe^{3+} to Fe^{2+} takes place. However, not all of the oxidized Fe^{2+} to Fe^{3+} ions were able to selectively oxidize benzene to phenol. This indicates that only a fraction of iron is catalytically active. For [Fe,Al]MFI catalysts with relatively high iron concentration, most of the extra-framework iron species formed are inactive in the direct oxidation of benzene to phenol. Finally, a more detailed in situ Mössbauer study for one sample, i.e. [Fe,Al]MFI (1:8) catalyst, was performed to illustrate the reduction/oxidation properties of the different iron species formed after steam-treatment.

Keywords: ^{57}Fe Mössbauer spectroscopy; Steam-activated [Fe,Al]MFI; Benzene oxidation to phenol

1. Introduction

Extra-framework iron species stabilized in the micropore channels of steam-activated isomorphously substituted [Fe,Al]MFI zeolite have attracted increasing attention due to their ability to catalyze different reactions [1–5]. One particular reaction of interest nowadays is the direct oxidation of benzene to phenol using N_2O as oxidant [6–8], which could potentially replace the three-step cumene process for the production of phenol.

Several methods have been reported [9–11] to introduce extra-framework iron species in the MFI zeolite. Nevertheless, the hydrothermal synthesis of isomorphously substituted [Fe,Al]MFI, followed by calcination, conversion to H-form, and finally steam-activation to remove the framework iron to extra-framework positions [6,8,12] appears to be the most promising route to form the active sites for the direct oxidation of benzene to phenol. Although there is still no agreement in literature as to the identity of the active sites, evidences are directing towards these extra-framework iron species as the catalytically active centers [13–17]. However, despite extensive efforts the structure and nuclearity of the active iron sites remain unknown. Much of the uncertainties in determining the nature of the active sites stem from diversities in preparation method, synthesis conditions, and elemental compositions, leading to various extra-framework iron species. Because of this, elucidation of the structure–activity relationships remains unclear. Therefore, it becomes essential for structure–activity studies to start with a relatively homogeneous form of extra-framework iron species.

* Corresponding author. Tel.: +31 15 2784597.
E-mail address: J.B.Taboada@iri.tudelft.nl (J.B. Taboada).

0920-5861/$ – see front matter
doi:10.1016/j.cattod.2005.09.036

Recently, we reported the formation of extra-framework iron species that are predominantly (ca. 90%) in the high-spin Fe^{2+} state after steam-activation [18]. Moreover, it was determined that the formation of these extra-framework Fe^{2+} species in the zeolite channels was independent of iron concentration (0.075–0.6 wt.% iron). In this contribution, we report the performance of these [Fe,Al]MFI catalysts in the direct oxidation of benzene to phenol. ^{57}Fe Mössbauer spectroscopy is used as the principal characterization technique to elucidate the different iron species formed after steam-activation. This technique is one of the most informative methods for studying iron containing solids since no form of iron is Mössbauer-silent, in contrast to electron paramagnetic resonance (EPR) spectroscopy. Moreover, iron species in different environments are observed, giving richer information compared to bulk averaging techniques such as magnetic susceptibility.

2. Experimental methods

2.1. Preparation of [Fe,Al]MFI

Due to low iron concentrations, the [Fe,Al]MFI zeolites need to be enriched with ca. 96% ^{57}Fe isotope since natural iron contains only 2 wt.% of this isotope. Fe-foil containing ca. 96% ^{57}Fe was used as the starting material, and the zeolites were prepared by hydrothermal synthesis with varying iron (0.075–0.6 wt.%) concentration as described in an earlier publication [19]. Table 1 gives a summary of all as-prepared samples with their molar compositions both in the synthesis gel and in the zeolite crystal. To remove the organic template in the as-prepared zeolites, the samples were calcined in air at 823 K for 10 h. The calcined zeolites were then transformed into the H-form by three consecutive exchanges with 0.1 M ammonium nitrate overnight and subsequent calcination at 823 K for 5 h. Finally, the samples were steam-activated at 873 K for 5 h, making them active in the one-step oxidation of benzene to phenol using N_2O as oxidant [6,8,12]. For this step, the reactor was equipped with a water-filled saturator that was kept at 343 K to obtain a water partial pressure of 300 mbar in 30 ml min^{-1} flow of He. After steam-activation, the samples were cooled to room temperature in inert atmosphere (i.e. 30 ml min^{-1} flow of He).

In all samples, calcination and steam-activation steps were carried out using a temperature ramp of 5 K/min.

2.2. Characterization techniques

The elemental analysis of the as-prepared zeolites was carried out by inductively coupled plasma optical emission spectroscopy (ICP-OES), Perkin-Elmer Plasma 40 (Si) and Optima 3000DV (axial) instruments.

^{57}Fe Mössbauer spectra were measured on a constant acceleration spectrometer in a triangular mode with a ^{57}Co:Rh source. Spectra for the different [Fe,Al]MFI samples were obtained at 300 K (both in air and in high vacuum, 10^{-6} mbar), and 77 and 4.2 K in high vacuum. The spectra were fitted with Lorentzian-shaped lines to obtain the Mössbauer parameters (i.e. isomer shift [IS], quadrupole splitting [QS], and hyperfine field [HF]). Isomer shift values are reported relative to sodium nitroprusside. The magnetically split lines were fitted with several components to simulate a distribution of hyperfine fields. Thus, the hyperfine field reported here is the average value and only the sum of the magnetically split components is shown in figures.

For in situ Mössbauer studies, a reactor equipped with a stainless steel cell with beryllium windows was used to avoid air exposure. Description of the reactor and the in situ cell is reported elsewhere [20]. A sample of about 160 mg of the catalyst is placed in the in situ cell and is subjected to different gas treatments at high temperature. The approach is to have a breakdown of the catalytic cycle and then measure the Mössbauer spectrum after every in situ treatment. That means: (1) after pretreatment with He flow of 30 ml/min at 823 K for 2 h; (2) after N_2O loading with 30 ml/min N_2O at 623 K for 1.5 h, and finally; (3) after reaction of benzene with N_2O using a flow rate of 30 ml/min (4/96, v/v of C_6H_6/N_2O) at 623 K for 1.5 h. The reaction was quenched by cooling to room temperature and then transferred to a cryostat under controlled environment for low temperature (i.e. 77 and 4.2 K) Mössbauer measurements.

Reaction data were collected in a single-pass atmospheric plug flow reactor. Typically, 100 mg of catalyst was diluted with an amount of SiC to obtain a catalyst bed of 2 cm in height. Gas-phase product analysis was performed by a well-calibrated combination of GC and MS. Prior to reaction, the catalyst was pretreated in a flow of 100 ml/min of He for 2 h at 823 K (using a heating rate of 1 K/min). Benzene oxidation was carried out by feeding a mixture of $C_6H_6/N_2O/He$ (1/4/95, v/v/v) at a flow rate of 100 ml/min at a reaction temperature of 623 K.

Table 1
Elemental composition of the various [Fe,Al]MFI zeolites based on ICP-OES

Sample	Si (wt.%)[a]	Al (wt.%)[a]	Fe (wt.%)[a]	Si/Al (mol/mol)[b]	Si/Fe (mol/mol)[b]	Si/Al (mol/mol)[c]	Si/Fe (mol/mol)[c]
[Fe,Al]MFI (1:4)	39.0	1.10	0.56	33	141	36	152
[Fe,Al]MFI (1:8)	39.0	1.16	0.28	33	279	36	300
[Fe,Al]MFI (1:16)	39.0	1.15	0.14	33	558	36	600
[Fe,Al]MFI (1:24)	39.0	1.10	0.10	34	794	36	900
[Fe,Al]MFI (1:32)	39.0	1.20	0.08	31	1018	36	1200

[a] Weight percent in the as-prepared zeolite.
[b] Molar ratio in the as-prepared zeolite.
[c] Molar ratio of the synthesis gel.

3. Results and discussion

3.1. Preparation of [Fe,Al]MFI zeolites

Five samples of [Fe,Al]MFI zeolites with varying iron concentration (0.075–0.6 wt.% Fe) were prepared as listed in Table 1. The amount of 0.6 wt.% iron in the isomorphously substituted [Fe,Al]MFI appears to be the upper limit in successfully incorporating all iron in the zeolite framework [19]. From 0.6 wt.% iron, the amount of iron was systematically decreased to 0.075 wt.% iron. As listed in Table 1, the molar compositions of silicon, aluminum, and iron in the as-prepared samples are very similar to their corresponding composition in the synthesis gel.

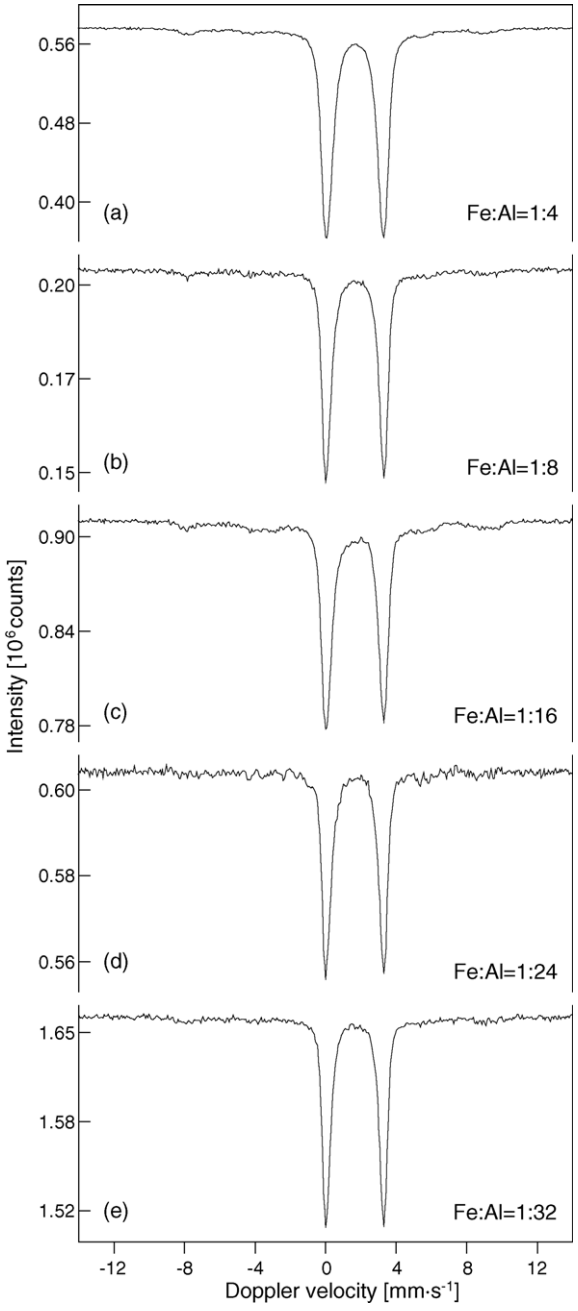

Fig. 1. ^{57}Fe Mössbauer spectra of steam-treated samples (a) [Fe,Al]MFI (1:4), (b) [Fe,Al]MFI (1:8), (c) [Fe,Al]MFI (1:16), (d) [Fe,Al]MFI (1:24), and (e) [Fe,Al]MFI (1:32), taken at 4.2 K in 10^{-6} mbar vacuum. The aluminum content in all samples is constant at 1.1 wt.%.

3.2. Steam-activation of [Fe,Al]MFI zeolites

The complete series of Mössbauer spectra of steam-activated samples with varying iron (0.075–0.6 wt.% iron keeping aluminum constant at 1.1 wt.%) concentration taken at 4.2 K are shown in Fig. 1. The spectra (Fig. 1a–e) of all samples exhibit a predominant doublet with an isomer shift of 1.67 mm s^{-1} and quadrupole splitting of 3.20 mm s^{-1} that is attributed to iron in high-spin Fe^{2+} state, ca. 90% based on spectral contribution (see Table 2). The Mössbauer parameters of the high-spin Fe^{2+} component are very similar to the high-spin Fe^{2+} complex observed by Panov and coworkers [21], which they attributed to binuclear iron complexes similar to those present in the enzyme methane monooxygenase (MMO). For these enzymatic complexes, almost equal Mössbauer parameters have been obtained [22]. MMO activates dioxygen for incorporation into a wide variety of hydrocarbons [23,24].

It is remarkable that all [Fe,Al]MFI catalysts in this study contain mostly Fe^{2+} ions after steam-activation, independent of iron concentration. This strongly emphasizes the critical nature of the steaming method, since hardly any divalent iron was observed in previous studies [8,12].

3.3. Catalytic activity of [Fe,Al]MFI catalysts

The rates of phenol formation expressed per gram of iron as a function of the reaction time for various [Fe,Al]MFI catalysts are shown in Fig. 2. The corresponding reaction data are condensed in Table 3. The phenol productivity is expressed per gram of iron since most iron species in the samples are in the Fe^{2+} state (>90%), which is proposed to be the state of iron in the active sites [13,17]. From Fig. 2, it is apparent that the catalyst activity per gram of iron increases as the iron concentration decreases. This indicates that only a fraction of iron is catalytically active in the direct oxidation of benzene to

Table 2
^{57}Fe Mössbauer parameters at 4.2 K of steam-treated [Fe,Al]MFI catalysts in Fig. 1

Spectrum no.	[IS] (mm s^{-1})	[QS] (mm s^{-1})	[HF] (T)	Relative intensity (%)	Oxidation state
1a	1.67	3.19		92	Fe^{2+}
	0.96		52.1	8	Fe^{3+}
1b	1.67	3.24		90	Fe^{2+}
	0.98		52.0	10	Fe^{3+}
1c	1.67	3.23		83	Fe^{2+}
	0.92		52.0	17	Fe^{3+}
1e	1.66	3.23		94	Fe^{2+}
	0.94		52.0	6	Fe^{3+}
1e	1.65	3.24		95	Fe^{2+}
	0.92		52.0	5	Fe^{3+}

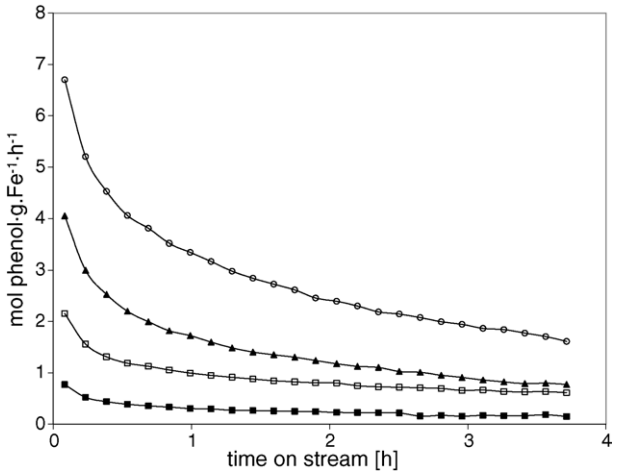

Fig. 2. Phenol productivities per gram iron as a function of reaction time of various steam-treated samples (■) [Fe,Al]MFI (1:4), (□) [Fe,Al]MFI (1:8), (▲) [Fe,Al]MFI (1:16), and (○) [Fe,Al]MFI (1:32). [Fe,Al]MFI (1:24) is similar to [Fe,Al]MFI (1:32), and is not shown.

phenol. Moreover, this fraction evidently increases with decreasing iron content.

Although the Mössbauer spectra of all samples (Fig. 1) show a single high-spin Fe^{2+} component, it is thus clear from the activity data that we are dealing with various iron species. These species are most likely a distribution of isolated extra-framework iron species to oligonuclear iron clusters, while no large iron oxide particles were detected by TEM [18]. The different iron species were discriminated by Mössbauer spectroscopy only after N_2O oxidation of the samples at 623 K (see Fig. 3). Fig. 3 shows that most Fe^{2+} species (>90% based on spectral contribution) were oxidized to various Fe^{3+} species in the presence of N_2O (Table 4). Because N_2O is a two-electron oxidant, which catalyzes the two-electron oxidation of benzene to phenol, this seems to indicate the presence of Fe^{3+}-dinuclear intermediates. However, since only a fraction of iron is catalytically active, this suggests that not all oxidized Fe^{2+} to Fe^{3+} species were able to generate active oxygen species needed for the oxidation of benzene to phenol.

To illustrate the reactivity of the generated oxygen species from N_2O towards benzene oxidation, the initial N_2O conversions and the initial phenol productivities as a function of the initial Fe^{2+} concentration are plotted in Fig. 4. In the figure, the amount of N_2O converted apparently increases with the increase in Fe^{2+} ions. This is because most of the Fe^{2+} ions

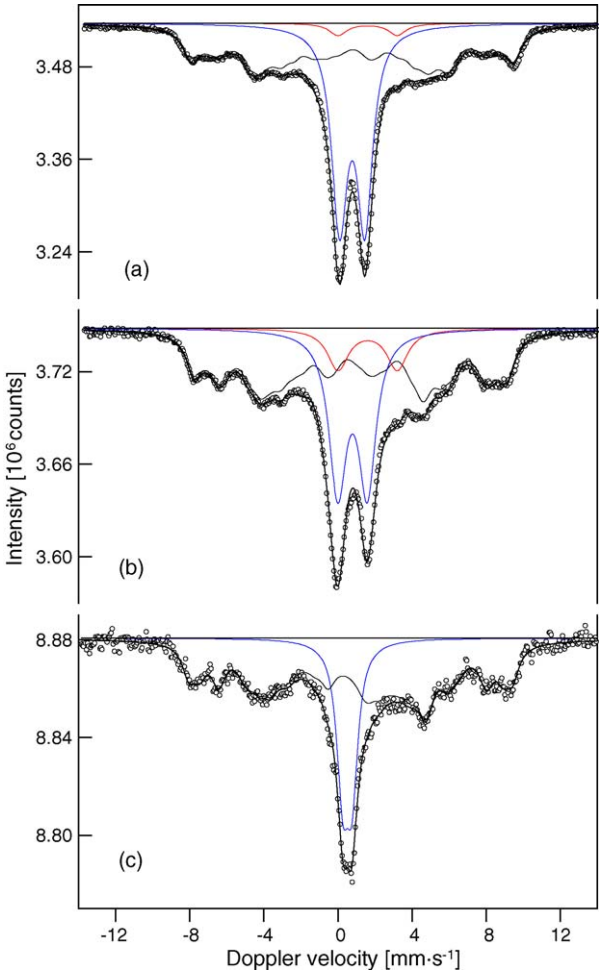

Fig. 3. ^{57}Fe Mössbauer spectra taken at 4.2 K of different samples after heat treatment in inert and N_2O oxidation at 623 K. (a) [Fe,Al]MFI (1:4); (b) [Fe,Al]MFI (1:8); and (c) [Fe,Al]MFI (1:32). Scattered open circles indicate experimental data. Solid line through data shows the fit, and remaining lines give the sub-spectra.

were oxidized to Fe^{3+} by N_2O, as shown above. However, in the same figure, the initial phenol productivities decreases with increasing iron concentration. This clearly demonstrates that for [Fe,Al]MFI catalysts the selectivity of converted N_2O towards phenol decreases with the increase in iron concentration. The decrease in selectivity of converted N_2O towards phenol can be attributed to overoxidation of benzene to condensable products like dihydroxybenzenes [25] as well as

Table 3
Reaction data of the [Fe,Al]MFI samples with varying iron concentration

Sample	t_R = 5 min				t_R = 4 h			
	$X_{C_6H_6}$	$S_{C_6H_6}$	X_{N_2O}	S_{N_2O}	$X_{C_6H_6}$	$S_{C_6H_6}$	X_{N_2O}	S_{N_2O}
[Fe,Al]MFI (1:4)	0.26	0.70	0.14	0.31	0.11	0.50	0.15	0.07
[Fe,Al]MFI (1:8)	0.37	0.70	0.12	0.54	0.10	>.99	0.03	0.70
[Fe,Al]MFI (1:16)	0.27	0.90	0.10	0.60	0.07	0.80	0.02	0.60
[Fe,Al]MFI (1:24)	0.29	0.92	0.11	0.65	0.07	>.99	0.02	>.99
[Fe,Al]MFI (1:32)	0.22	0.80	0.10	0.50	0.07	0.70	0.01	0.80

Data contains benzene conversions ($X_{C_6H_6}$), benzene selectivities to phenol ($S_{C_6H_6}$), nitrous oxide conversions (X_{N_2O}), and nitrous oxide selectivities to phenol (S_{N_2O}) after reaction times (t_R) of 5 min and 4 h.

Table 4
^{57}Fe Mössbauer parameters at 4.2 K of N_2O-treated [Fe,Al]MFI catalysts in Fig. 3

Spectrum no.	[IS] (mm s^{-1})	[QS] (mm s^{-1})	[HF] (T)	Relative intensity (%)	Oxidation state
3a	1.60	3.20		3	Fe^{2+}
			54.3	53	Fe^{3+}
3b/4c	0.76	1.37		44	Fe^{3+}
	1.60	3.20		10	Fe^{2+}
			48.4	57	Fe^{3+}
3c	0.78	1.59		33	Fe^{3+}
	0.51	0.50		25	Fe^{3+}
			54	75	Fe^{3+}

coke formation [26] and deep oxidation to CO_x. The latter is confirmed by the formation of CO_2 and H_2O in the product stream as detected by mass spectroscopy specifically for the catalyst with relatively high iron concentration (0.6 wt.%).

It is evident from Mössbauer spectroscopy that for samples with relatively high iron content, the formation of large clusters of extra-framework iron ions is favorable. This is denoted in the spectra by the presence of a fully relaxed high-spin Fe^{3+} doublet [18,27] (see Fig. 3a). However, these species apparently provide low selectivity towards phenol. On the other hand, for low iron concentrations, e.g. [Fe,Al]MFI (1:32), the spectrum exhibits paramagnetic hyperfine splitting [28] suggesting large Fe–Fe distances typical for highly dispersed iron species. Thus, the observation in this study that the activity apparently increases with decreasing iron concentration indicates that highly dispersed extra-framework iron species are the active centers in N_2O-mediated oxidation of benzene to phenol.

3.4. In situ Mössbauer study of [Fe,Al]MFI catalyst

To better understand the redox properties of the different iron species formed after steam-activation, in situ Mössbauer study of the steam-activated [Fe,Al]MFI (1:8) was performed (see Section 2.2, for details). This sample was chosen for in situ study because it exhibits high benzene to phenol selectivity, and relatively high N_2O to phenol selectivity, at steady-state conditions (see Fig. 2 and Table 3).

The Mössbauer spectra at room temperature (77 K), and 4.2 K were taken after each in situ treatment. For brevity, only the spectra obtained at 4.2 K are presented and are shown in Fig. 5, with their corresponding parameters listed in Table 5. For the untreated steamed catalyst (Fig. 5a), three components were observed. For discussion purposes, we assign the components observed as type I, which is typical for octahedrally coordinated extra-framework Fe^{3+} ions; type II, which is the high-spin Fe^{2+} component with parameters similar to that of the Panov catalyst; and type III, which we attribute to

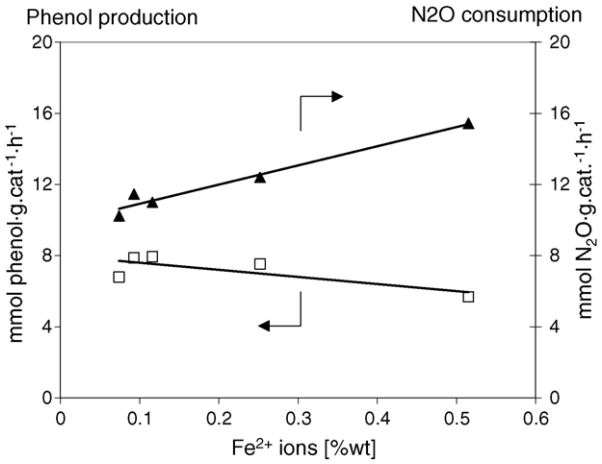

Fig. 4. (▲) Initial N_2O conversions and (□) initial phenol productivities as a function of Fe^{2+} ions (wt.%) in various steam-treated samples.

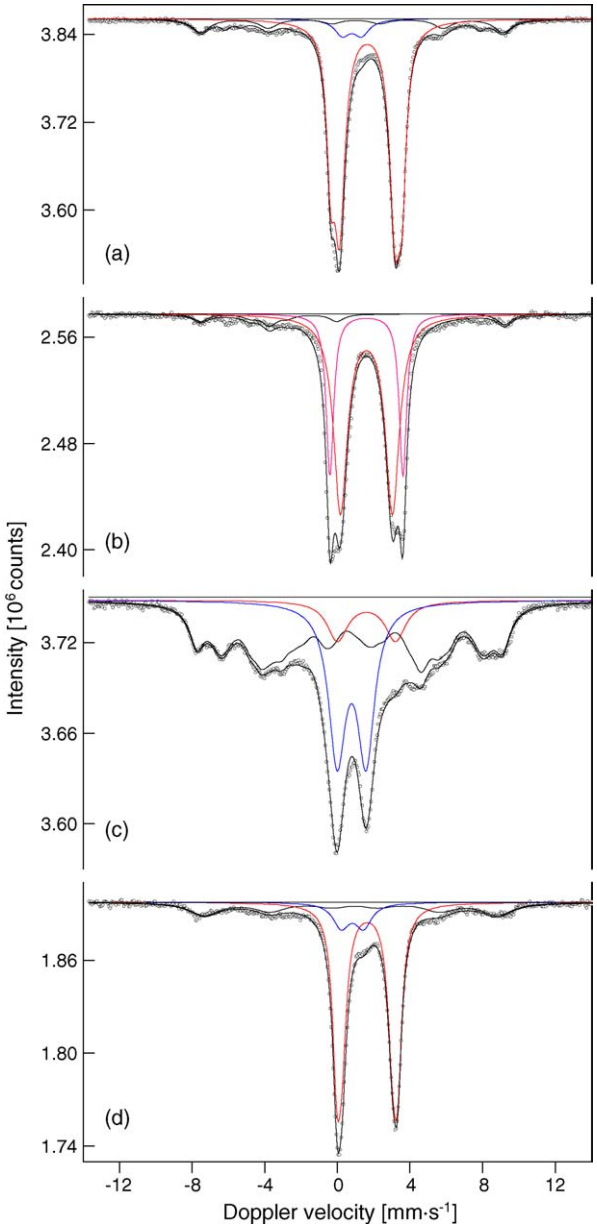

Fig. 5. ^{57}Fe Mössbauer spectra taken at 4.2 K of (a) steam-treated [Fe,Al]MFI (1:8) catalyst, (b) after pretreatment in He, (c) after loading with N_2O, and (d) after reaction with benzene in excess N_2O. Scattered open circles indicate experimental data. Solid line through data shows the fit, and remaining lines give the sub-spectra.

Table 5
^{57}Fe Mössbauer parameters at 4.2 K of in situ treated [Fe,Al]MFI (1:8)$_{stm}$ (see Fig. 5)

Spectrum no.	Component	I.S. (mm s^{-1})	Q.S. (mm s^{-1})	H.F. (T)	Contribution (%)	Oxidation
5a	I	0.80	1.06		6	Fe^{3+}
	II	1.60	3.20		79	Fe^{2+}
	III	0.90		52.0	15	Fe^{3+}
5b	IIa	1.60	3.90		28	Fe^{2+}
	IIb	1.60	2.80		64	Fe^{2+}
	III			50.4	8	Fe^{3+}
5c	II	1.60	3.20		10	Fe^{2+}
	IIIa			48.4	57	Fe^{3+}
	IV	0.78	1.59		33	Fe^{3+}
5d	I	0.80	1.22		11	Fe^{3+}
	II	1.64	3.36		68	Fe^{2+}
	III	0.84		50.4	21	Fe^{3+}

^{57}Fe Mössbauer parameters isomer shift (I.S.), quadrupole splitting (Q.S.), and hyperfine field (H.F.) are given as well as the components oxidation state and their relative intensities based on spectral contribution (%).

paramagnetic hyperfine splitting of highly dispersed extra-framework Fe^{3+} ions. The latter is concluded, since no evidences of superparamagnetic iron oxide particles were found by TEM [18]. It should be noted that the spectrum of the untreated steamed catalyst (Fig. 5a) contains less Fe^{2+} ions with a broader linewidth compared to the spectrum of the freshly steamed catalyst (Fig. 1b). This is attributed to slow oxidation of some of the Fe^{2+} ions upon exposure to air for a considerable time (i.e. several weeks).

After pretreatment with He, we observed a splitting of the type II component into types IIa and IIb (see parameters in Table 5), which is a corroboration to a previous publication reported by some of us [29]. This implies that the Fe^{2+} sites in the steam-treated [Fe,Al]MFI are not identical. Therefore, we doubt the hypothesis of Panov and coworkers regarding the structure of the Fe^{2+} species (vide supra).

Upon oxidation of the pretreated sample with N_2O, essentially all Fe^{2+} ions were oxidized to the Fe^{3+} state. A new high-spin Fe^{3+} component is formed and assigned as type IV (see Table 5). Since type IV gives a fully relaxed high-spin Fe^{3+} doublet at 4.2 K, this component can be assigned to small clusters of Fe^{3+} ions. The rest of the Fe^{3+} ions, mostly from the oxidation of type IIb, sums up into a complicated magnetically split pattern, hereafter referred to as type IIIa. Due to the complicated nature of type IIIa, it is rather difficult to discriminate the different forms of magnetically split iron species. Nonetheless, the complicated magnetically split pattern can be attributed to paramagnetic hyperfine splitting of highly dispersed extra-framework Fe^{3+} ions in different environments.

Finally, after steady-state reaction with benzene in the presence of excess N_2O at 623 K, the oxidized-form of the catalyst is reverted to its reduced form as indicated by the Mössbauer spectrum (Fig. 5d). This indicates that the Fe^{3+} ions that form the type IV and the complicated magnetically split type IIIa components were reduced in the presence of benzene. It is remarkable that under steady-state reaction conditions, most of the extra-framework iron species were present in the high-spin Fe^{2+} state. Since >90% of the Fe^{2+} species were oxidized to the Fe^{3+} state in the presence of N_2O, and roughly 2/3 of the Fe^{3+} ions revert to Fe^{2+} ions, this implies that about 60% of the total iron in the [Fe,Al]MFI (1:8) sample was involved in the catalytic reaction (see Table 5).

However, although this study shows that the direct oxidation of benzene to phenol, using N_2O as oxidant is accompanied by an oxidation of Fe^{2+} to Fe^{3+} followed by the reduction of the Fe^{3+} to Fe^{2+} ions, it is not clear at the moment, which Fe^{3+} species are affected in the reduction step due to phenol desorption only. Therefore, for the structure–activity study, it becomes crucial to have a better discrimination of the active iron species. This could be achieved by suppressing the contribution of the unwanted reduction reactions, by lowering the iron concentration and the reaction temperature in a single turnover benzene experiment.

4. Conclusions

The performance of various [Fe,Al]MFI catalysts, containing ca. 90% of extra-framework iron in the high-spin Fe^{2+} state has been evaluated in the direct oxidation of benzene to phenol with N_2O as oxidant. From Mössbauer data, most Fe^{2+} species (>90%) were oxidized to Fe^{3+} species by N_2O, independent of iron concentration (0.075–0.6 wt.%). However, we stress that only a fraction of the oxidized Fe^{2+} to Fe^{3+} species was able to generate the ‘‘active’’ oxygen for the oxidation of benzene to phenol. This fraction increases with deceasing iron concentration.

Although Mössbauer spectra of steam-activated samples suggest the formation of a single high-spin Fe^{2+} complex, in situ treatments under oxidizing and reducing environments reveal that a distribution of Fe^{2+} species is present. At relatively high iron concentrations, most likely large extra-framework iron clusters are formed that exhibit low benzene and N_2O selectivity towards phenol. Finally, the observation in this study that the activity apparently increases with decreasing iron concentration is directing towards the hypothesis that highly dispersed extra-framework iron sites are the active centers in the one-step oxidation of benzene to phenol.

References

[1] A.A. Battiston, J.H. Bitter, D.C. Koningsberger, Catal. Lett. 66 (2000) 75.
[2] L.J. Lobree, I. Hwang, J.A. Reimer, A.T. Bell, Catal. Lett. 63 (1999) 233.
[3] H.-Y. Chen, T. Voskoboinikov, W.M.H. Sachtler, J. Catal. 180 (1998) 171.
[4] E.M. El-Malki, R.A. van Santen, W.M.H. Sachtler, J. Catal. 196 (2000) 212.
[5] F. Kapteijn, G. Marbán, J. Rodríguez-Mirasol, J.A. Moulijn, J. Catal. 167 (1997) 256.
[6] G.I. Panov, Cattech 4 (2000) 18.
[7] P.P. Notté, Top. Catal. 13 (2000) 387.
[8] A. Ribera, I.W.C.E. Arends, S. de Vries, J. Pérez-Ramírez, R.A. Sheldon, J. Catal. 195 (2000) 287.
[9] X. Feng, W.K. Hall, J. Catal. 166 (1997) 368.
[10] C. Plog, F. Schueth, V. Goeman, R. Andorf, Preparation of a Fe- or Mn-Exchanged Zeolite, EP 0867406, 1998.
[11] M. Kögel, V.H. Sandoval, W. Schwieger, A. Tissler, T. Turek, Catal. Lett. 51 (1998) 23.
[12] J. Pérez-Ramírez, G. Mul, F. Kapteijn, J.A. Moulijn, A.R. Overweg, A. Doménech, A. Ribera, I.W.C.E. Arends, J. Catal. 207 (2002) 113.
[13] K.A. Dubkov, N.S. Ovanesyan, A.A. Shteinman, E.V. Starokon, G.I. Panov, J. Catal. 207 (2002) 341.
[14] A.M. Ferretti, C. Oliva, L. Forni, G. Berlier, A. Zecchina, C. Lamberti, J. Catal. 208 (2002) 83.
[15] J.A. Ryder, A.K. Chakraborty, A.T. Bell, J. Catal. 220 (2003) 84.
[16] J. Pérez-Ramírez, F. Kapteijn, A. Brückner, J. Catal. 218 (2003) 234.
[17] P.K. Roy, G.D. Pirngruber, J. Catal. 227 (2004) 164.
[18] J.B. Taboada, A.R. Overweg, P.J. Kooyman, I.W.C.E. Arends, G. Mul, J. Catal. 231 (2005) 56.
[19] J.B. Taboada, A.R. Overweg, M.W.J. Crajé, I.W.C.E. Arends, G. Mul, A.M. van der Kraan, Microporous Mesopororous Mater. 75 (2004) 237.
[20] J.W. Niemantsverdriet, C.F.J. Flipse, A.M. van der Kraan, J.J. van Loef, Appl. Surf. Sci. 10 (1982) 302.
[21] N.S. Ovanesyan, A.A. Shteinman, K.A. Dubkov, V.I. Sobolev, G.I. Panov, Kinet. Catal. 39 (1998) 792.
[22] J.G. DeWitt, J.G. Bentsen, A.C. Rosenzweig, B. Hedman, J. Green, S. Pilkington, G.C. Papaeftymiou, H. Datlton, K.O. Hodgson, S.J. Lippard, J. Am. Chem. Soc. 113 (1991) 9219.
[23] J. Green, H. Dalton, J. Biol. Chem. 264 (1989) 17698.
[24] B.G. Fox, J.G. Borneman, L.P. Wackett, J.D. Lipscomb, Biochemistry 29 (1990) 6419.
[25] Q. Zhu, R.M. van Teeffelen, R.A. van Santen, E.J.M. Hensen, J. Catal. 221 (2004) 575.
[26] D. Meloni, R. Monaci, V. Solinas, G. Berlier, S. Bordiga, I. Rossetti, C. Oliva, L. Forni, J. Catal. 214 (2003) 169.
[27] A. Meagher, V. Nair, R. Szostak, Zeolites 8 (1988) 3.
[28] S. Mørup, J.E. Knudsen, M.K. Nielsen, G. Trumpy, J. Chem. Phys. 65 (1976) 536.
[29] A.R. Overweg, M.W.J. Crajé, A.M. van der Kraan, I.W.C.E. Arends, A. Ribera, R.A. Sheldon, J. Catal. 223 (2004) 262.